


Multimomics, virtual reality and artificial intelligence in heart failure

Patrick A Gladding^{*1} , Suzanne Loader¹, Kevin Smith², Erica Zarate³, Saras Green³, Silas Villas-Boas³, Phillip Shepherd⁴, Purvi Kakadiya⁴, Will Hewitt⁵, Eric Thorstensen⁶, Christine Keven⁶, Margaret Coe⁶, Bahareh Nakisa⁷, Tan Vuong⁷, Mohammad Naim Rastgoo⁸, Mia Jüllig⁹, Vito Starc¹⁰ & Todd T Schlegel^{11,12}

¹Department of Cardiology, Waitemata District Health Board, Auckland 0620, New Zealand

²Clinical Laboratory, Waitemata District Health Board, Auckland 0620, New Zealand

³School of Biological Science, University of Auckland, Auckland 1010, New Zealand

⁴Grafton Genomics Ltd, Liggins Institute, University of Auckland, Auckland 1023, New Zealand

⁵Auckland Bioengineering Institute, University of Auckland, Auckland 1010, New Zealand

⁶Liggins Institute, University of Auckland, Auckland 1023, New Zealand

⁷School of Information Technology, Deakin University, Victoria 3125, Australia

⁸School of Electrical Engineering & Computer Science, Queensland University of Technology, Brisbane, QLD 4072, Australia

⁹Paper Dog Limited, Waiheke Island, Auckland 1081, New Zealand

¹⁰Faculty of Medicine, University of Ljubljana, Ljubljana 1000, Slovenia

¹¹Karolinska Institutet, Stockholm, Sweden 171 77, Switzerland

¹²Nicollier-Schlegel Sàrl, Trélex, Karolinska 1270, Switzerland

*Author for correspondence: patrick.gladding@waitematadhb.govt.nz

Aim: Multimomics delivers more biological insight than targeted investigations. We applied multimomics to patients with heart failure (HF) and reduced ejection fraction (HFrEF), with machine learning applied to advanced ECG (AECG) and echocardiography artificial intelligence (Echo AI). **Patients & methods:** In total, 46 patients with HFrEF and 20 controls underwent metabolomic profiling, including liquid/gas chromatography–mass spectrometry and solid-phase microextraction volatilomics in plasma and urine. HFrEF was defined using left ventricular (LV) global longitudinal strain, EF and N-terminal pro hormone BNP. AECG and Echo AI were performed over 5 min, with a subset of patients undergoing a virtual reality mental stress test. **Results:** A-ECG had similar diagnostic accuracy as N-terminal pro hormone BNP for HFrEF (area under the curve = 0.95, 95% CI: 0.85–0.99), and correlated with global longitudinal strain ($r = -0.77$, $p < 0.0001$), while Echo AI-generated measurements correlated well with manually measured LV end diastolic volume $r = 0.77$, LV end systolic volume $r = 0.8$, LVEF $r = 0.71$, indexed left atrium volume $r = 0.71$ and indexed LV mass $r = 0.6$, $p < 0.005$. AI-LVEF and other HFrEF biomarkers had a similar discrimination for HFrEF (area under the curve AI-LVEF = 0.88; 95% CI: -0.03 to 0.15; $p = 0.19$). Virtual reality mental stress test elicited arrhythmic biomarkers on AECG and indicated blunted autonomic responsiveness (alpha 2 of RR interval variability, $p = 1 \times 10^{-4}$) in HFrEF. **Conclusion:** Multimomics-related machine learning shows promise for the assessment of HF.

Lay abstract: Multimomics is the integration of multiple sources of health information, for example, genomic, metabolite, etc. This delivers more insight than targeted single investigations and provides an ability to perceive subtle individual differences between people. In this study we applied multimomics to patients with heart failure (HF) using DNA sequencing, metabolomics and machine learning applied to ECG echocardiography. We demonstrated significant differences between subsets of patients with HF using these methods. We also showed that machine learning has significant diagnostic potential in identifying HF patients more efficiently than manual or conventional techniques.

First draft submitted: 14 December 2020; Accepted for publication: 6 May 2021; Published online: 19 May 2021

Keywords: artificial intelligence • metabolomics • multimomics • volatilomics

New diagnostic and management tools are needed for the emerging epidemic of heart failure (HF). While the introduction of blood-based biomarkers, such as N-terminal pro hormone BNP (NTproBNP), has improved diagnosis of HF in the community, more work is needed to identify the causes of HF, stratify the syndrome into its subtypes for targeted therapies and identify patients at higher risk for adverse events, such as ventricular arrhythmia. As containment of healthcare costs has become paramount, increased efficiency must also be achieved with often diminishing resources, and with a strong emphasis on portability and accessibility. The emergence of low cost sensors, ubiquitous computing and the internet of things, as well as artificial intelligence (AI) applied to hospital data hold promise for addressing both individual and population scale diagnostic and treatment gaps [1].

Deep phenotyping with multiomics, combined with AI applied to wearable devices and existing clinical data, holds considerable promise in identifying novel low-cost biomarkers and intermediate endophenotypes for early disease stratification and prognostication [2]. Deep learning, using convolutional neural networks, applied to digital ECG is one of the more promising applications of AI in HF [3,4]. However it lacks the transparency and explainability required to stratify patients and identify disease mechanisms. We have shown that a machine learning model applied to digital 12L ECG can identify moderate to severe left ventricular systolic dysfunction (LVSD) [5] with a similarly high degree of accuracy. As the method is transparent, it also reports a number of well validated ECG biomarkers of arrhythmia including the spatial QRS-T angle [6]. Stratification of HF patients by the spatial QRS-T angle and other discrete parameters identifies those at higher risk for HF readmission, implantable cardioverting defibrillator (ICD) implantation and death [6]. Deep learning applied to echocardiography has also been shown to both accurately classify views and LV ejection fraction (LVEF), chamber volumes, LV mass, global longitudinal strain (GLS) and diagnoses [7–9]. Furthermore AI has been shown to also assist echocardiography image acquisition by probe guidance [10]. With these tools, AI-enabled unskilled users could potentially use point of care ultrasound (POCUS) to diagnose HF and its most likely cause.

Wearable devices have the advantage of gathering longitudinal data from continuous monitoring rather than from episodic hospital encounters. The LINK-HF study showed that personalized AI modeling applied to data from a single lead ECG patch accurately identified patients 6–7 days prior to readmission with HF [11]. The advantage of wearable sensors is that a wide range of activities are captured within the context of life events including, for example, walking pace, sleep, exercise and stress. Mental stress is of considerable interest as not only has it been shown to have a significant negative impact on cardiovascular health, for example, Takotsubo syndrome, but similar to an exercise stress test mental stress can be applied in a standardized fashion. Integrating multiomics data across multiple domains such as metabolomics, advanced ECG (AECG), echocardiography and mental stress testing with wearable devices is complex but achievable.

We therefore undertook an investigation of the utility of multiomics and deep phenotyping in patients with HF with reduced EF (HFrEF) using AI and machine learning applied to standard clinical data. In a subset of HF patients and controls, we also applied a standardized virtual reality mental stress test (VR-MS), using validated methods, to evaluate stress biometrics from a wearable device and arrhythmic biomarkers identified by AECG. The primary objective was to evaluate the diagnostic accuracy of AECG and echocardiography AI (Echo AI) in patients with HF. The secondary objective was to explore the biophysical response to a standardized VR-MS. We hypothesized that advanced diagnostic tools utilizing machine learning would accurately discriminate HF from healthy controls, and demonstrate the proarrhythmic effects of mental stress in patients with HF.

Patients & methods

Patients

The NanoHF study was approved by the Northern B Health and Disability Ethics Committee (16/NTB/115) (#16/680) and Waitematā District Health Board's IRB (#RM13458). Patients with HFrEF were identified from an echocardiography database, >18 years of age, able to provide written informed consent, and had previously documented signs and symptoms of HF with an EF from 20 to 45% on echocardiography. Exclusion criteria included: diabetes mellitus (Type 1, Type 2 on insulin and/or last available HbA1c ≥ 65 mmol), chronic renal impairment (estimated glomerular filtration rate [eGFR] <50 ml/min), chronic lung disease (e.g., chronic obstructive airways disease [COPD] and asthma) and/or hospital admission within 3 months of enrolment related to exacerbation of HF. HF was defined as a clinical syndrome with biochemical (NTproBNP >212 pmol/l at any age; normal <35 pmol/l), mechanical (LVEF <50% or GLS <18%) or electrical (using a validated AECG score [12]) evidence

for HFref. Enrolment was enriched for patients with devices (ICD and cardiac resynchronization therapy). Controls were self-reported volunteers who also underwent ECG and echocardiography. Recovered HF (HFrec) was defined biochemically, NTproBNP <35 pmol/l, or mechanically GLS \geq 18% or LVEF \geq 50%.

Biomarkers & genomics

Blood was collected using ethylenediaminetetraacetic acid tubes. After centrifugation at $3000 \times g$ for 5 min, plasma was stored at -80°C before being shipped on dry ice to core lab facilities for testing. NTproBNP was measured using a Siemens Dimension Vista assay. First morning urinary levels of titin-N-terminal fragments (U-TTN) were measured by a highly sensitive sandwich ELISA (#27900 Titin N-Fragment Assay Kit, Immuno-Biological Laboratories, Gunma, Japan) system [13]. To avoid effects of concentration or attenuation of urine, the value of titin N-fragment concentration was corrected by the value of creatinine, and expressed by the following creatinine ratio: (U-TTN/Cr; pmol/ $\mu\text{mol/l}$), as previously described [13].

Metabolomics

Plasma and urine samples underwent gas chromatography–mass spectrometry analysis using a methyl chloroformate derivatization, and solid-phase microextraction (SPME) volatilomics using an Agilent 7890A gas chromatograph coupled to a 5975C inert mass spectrometer. Plasma samples were analyzed using targeted liquid chromatography–mass spectrometry. A metabolomics approach was used to analyze plasma samples from HFref patients and controls via an AbsoluteIDQ p400 kit (Biocrates Life Sciences AG, Innsbruck, Austria) using a Thermo Q-Exactive Orbitrap liquid chromatography–mass spectrometry. SPME results were validated using a Ketoscan mini (Sentech, Gyeonggi-Do, Korea) in a sample of cardiac inpatients and outpatients.

DNA sequencing

DNA was extracted from buffy coat and underwent sequencing of 174 genes associated with inherited cardiac disease using the Cardiac Trusight panel on an Illumina MiSeq (Grafton Genomics, Auckland, New Zealand). Cardioclassifier (<https://www.cardioclassifier.org/> [Imperial College London, 2017]) was used for variant calling.

Advanced ECG

ECGs were recorded using a Cardiac machine (Imed, Budapest, Etele, Hungary). AECG analyzed parameters included those derived from the conventional scalar 12-lead ECG, as well as from signal averaging of all adequately cross-correlated QRS and T complexes by using software originally assembled at NASA [12,14] to generate results for: several spatial (derived vectorcardiographic or 3D) ECG parameters including the spatial mean and peaks QRS-T angles, the spatial ventricular gradient, and various spatial waveform azimuths, elevations and time-voltages [12,15]; parameters of QRS and T-waveform complexity derived by singular value decomposition including the principal component analysis ratio [14], the dipolar and nondipolar voltage equivalents [16] of the QRS and T waveforms, and a parameter describing the shape of the T wave via measurement of the spatial allocation of equivalent dipoles that uses an error function to minimize the difference between measured and equivalent dipoles-reconstructed potentials, known as the root-normalized mean square error of the T wave (RNMSE-T) [17]. Data from the 5-min ECGs were also processed for multiple measures of both beat-to-beat RR and QT interval variability [18]. All AECG parameters have been described in previous publications [14,15,19]. We utilized a previously validated AECG score for using a validated multivariate logistic regression based on larger dataset of patients with known LVSD [5,12].

Echocardiography

A brief 5-min echocardiography protocol was used by a sonographer using a GE E95 to obtain standard measures such as LVEF using Simpson's biplane method. LVSD by echocardiography was considered present when LVEF <50%. LV GLS was also measured using EchoPAC (GE, IL, USA). DICOM files were fed into an AI pipeline to classify, segment and analyze each image. A convolutional neural network, described elsewhere [7], was used to label each view into one of 23 classes. The area-length formula was used to calculate AI-generated LV volumes (LVEDV/LVESV) and EF (AI-LVEF). AI-generated indexed LA volume and indexed LV mass were also compared with manual measurements (M). This pipeline is part of the integrated cardiac and modeling and analysis platform developed at the Auckland Bioengineering Institute (Integrated Cardiovascular Project, NSBRI Foundation, NASA Grant NCC 9-58) [20].

Table 1. Baseline characteristics.

	Heart failure (n = 46)	Controls (n = 20)	p-value
Age (years), mean (SD)	68 (8)	52 (9)	5×10^{-9}
Males, n (%)	41 (89)	10 (50)	0.0006
European, n (%)	29 (63)	16 (80)	0.18
AF, n (%)	10 (22)	0 (0)	N/A
HTN, n (%)	21 (46)	0 (0)	N/A
T2DM, n (%)	9 (20)	0 (0)	N/A
ACEi/ARB, n (%)	37 (80)	0 (0)	N/A
β -blocker, n (%)	39 (85)	0 (0)	N/A
MRA, n (%)	14 (30)	0 (0)	N/A
Statin, n (%)	29 (63)	0 (0)	N/A
Furosemide, n (%)	10 (22)	0 (0)	N/A
EF bp, mean (SD)	39% (10)	57% (5)	8×10^{-9}
GLS, mean (SD)	-13% (0.04)	-21% (0.05)	3×10^{-8}
NTproBNP (pmol/l), mean (SD)	115 (124)	8 (10)	0.0002

ACEi: Angiotensin converting enzyme inhibitor; AF: Atrial fibrillation; ARB: Angiotensin receptor blocker; EF bp: Ejection fraction by Simpson's biplane; GLS: Global longitudinal strain; HTN: Hypertension; MRA: Mineralocorticoid receptor antagonist; NTproBNP: N-terminal pro hormone BNP; SD: Standard deviation; T2DM: Type 2 diabetes.

Mental stress testing & wearable devices

A 3D VR-MS was created using validated content to evoke mental stress in a subset of participants with continuous AECG recording [21–23]. The content was based on a social trier stress test, serial subtraction, agoraphobic and other environmental stressors, designed to cause episodic mental stress, that have been associated with LV dysfunction [23] and arrhythmia [24], over a 5-min interval ([Supplementary Video 1](#)). VR epochs are listed in [Supplementary Table 1](#). A Samsung Gear VR headset with a Galaxy S8 was used with content run in Oculus. VR-MS participants wore an Empatica E4 on their dominant wrist, measuring skin temperature, electrodermal activity (EDA) and pulse photoplethysmography (PPSG). AECG was recorded 5-min prior and during VR-MS. A further 12 participants wore a radial pulse wave tonometer built by Microsoft Research, which included a single-lead 5-min ECG at baseline. EDA and PPSG signals were fed to an AI pipeline involving feature extraction from each channel consisting of mean, median, standard deviation, and min and max of data. Subsequently, all the extracted features from each channel (EDA, PPSG and combined signals) were concatenated into a single vector feature. The feature vector from these signals were fed into two classifiers, long short-term memory and support vector machine to distinguish between groups and within groups, before and during VR-MS.

Statistics

Univariate analysis was performed using the Student's *t*-test for continuous parametric variables, a Mann–Whitney *U*-test for nonparametric and chi-square test for categorical variables. Receiver operating characteristic curve analysis was used to assess performance of diagnostic biomarkers by *c*-statistic. All tests were two-tailed with $p < 0.05$ deemed statistically significant, except where tests for multiplicity were applied. Metaboanalyst (Version 4.0, Alberta, Canada) was used for pathway and multivariate analysis which was adjusted for multiplicity to reduce the false discovery rate (FDR). Medcalc software version 16.8.4 was used to analyze the data. The data output from mental stress testing were analyzed using GraphPad Prism 8 (version 8.4.3), comparing slopes, intercepts and elevations using simple linear regression.

Data availability

The materials, data, code and associated protocols are available to readers with application to the corresponding author.

Results

Three hundred and sixty two patients were screened for inclusion/exclusion criteria. Sixty six participants (46 with documented diagnosis of HF and 20 self-reported healthy volunteers) were enrolled in the study, with written informed consent. Baseline characteristics are outlined in [Table 1](#). Within HF patients 27 (59%) had an ischemic cardiomyopathy and 19 (41%) had either an ICD ($n = 14$) or cardiac resynchronisation therapy defibrillator

Table 2. Dilated cardiomyopathy pathogenic mutations.

Gene	Titin band	Coding HGVS	Genomic position	Zygosity	Variant type
<i>Titin</i>	A-band	c.96904+2T>A	chr2:179407794	Het	Splice donor variant
<i>Titin</i>	A-band	c.50296C>T	chr2:179476842	Het	Nonsense
<i>Titin</i>	I-band	c.43382delA	chr2:179497350	Het	Frameshift
<i>Titin</i>	M-band	c.101689G>T	chr2:179399653	Het	Nonsense
<i>Desmoplakin</i>	–	c.6805_6824delAAACAGAAGCTTGCCATTTA	chr6:7584298	Het	Frameshift

chr: Chromosome; del: Deletion; HGVS: Human Genome Variation Society.

therapy (CRTD; $n = 5$). Ten (71%) of the ICDs were implanted for primary prevention. HF patients were older and had a higher percentage of males than controls. Mean NYHA status was II.

Although patients were screened according to the criteria noted above based on historic data, a number of patients with HFrEF had recovered (HFrec) either spontaneously or with medical interventions. Seventeen (36%) had an NTproBNP <35 pmol/l and were defined as biochemical HFrec. Seven (15%) had mechanical HFrec, defined as GLS $\geq 18\%$ and 7 (15%) had LVEF $\geq 50\%$.

Biomarkers & genomics

28 metabolites across all diagnostic definitions of heart failure were identified by GCMS, which met false discovery rate (FDR). Numerous of these were either directly part of or indirectly linked to the citric acid cycle and mitochondrial metabolism. By univariate analysis, isocitric acid had the highest AUC 0.84, 95% CI 0.73 to 0.92 to discriminate HF. 35 metabolites were identified by LCMS which fulfilled the FDR. Most notably these included symmetric dimethyl arginine, creatinine, arginine and kynurenine, as well as numerous phosphatidylcholines, sphingomyelins, lysophosphatidylcholines, two cholesteryl esters and one triglyceride (55:9). Only one volatile, acetone, reached significance by the stringent FDR used, however several common VOCs were identified in both plasma and urine (t-test, $P < 0.05$) which have previously been associated with heart failure. These included pentane, 2-butanone, and 2-pentanone. Breath acetone was validated as a heart failure biomarker ($n = 61$) using a commercially available device (Ketoscan mini, Sentech, Gyeonggi-Do, Korea) with AUC of 0.8, 95% CI 0.61 to 0.92. Five (11%) patients had pathogenic mutations associated with dilated cardiomyopathy (Table 2), with four (9%) having *Titin* gene (*TTN*) truncations (*TTN*tv). U-*TTN*/Cr concentrations were statistically higher in patients with prior history of HF compared with controls (median 542 vs 360 pmol/ μ mol/l; difference 95% CI: 62–368; $p < 0.005$). In *TTN*tv carriers, U-*TTN*/Cr was not significantly different, though NTproBNP was substantially higher than in *TTN* wild-type HF patients (mean 347 vs 95 pmol/l; 95% CI: 144–359; $p < 0.0001$). Both kynurenine and hexanal, an aldehyde bioproduct of lipid peroxidation, were different ($p < 0.05$) in *TTN*tv carriers, but neither exceeded the statistical FDR.

Advanced ECG

The AECG LVSD score correlated with GLS ($r = -0.77$, $p < 0.0001$) as also previously demonstrated [6]. Moreover, it discriminated HF at baseline (area under the curve [AUC]: 0.95, 95% CI: 0.85–0.99) independent of NTproBNP (Figures 1 & 2), which itself correlated with cardiac energetics, not mechanics. QT variability index was higher in ischemic versus nonischemic cardiomyopathy ($p = 0.003$), especially in those with an ICD ($p = 0.0004$). Biochemical HFrec, defined by NTproBNP <35 pmol/l, was best discriminated by GLS (AUC: 0.84; 95% CI: 0.68–0.94; $p < 0.0001$), urine creatinine (AUC: 0.81; 95% CI: 0.67–0.93; $p = 1 \times 10^{-5}$) and plasma acetone (AUC: 0.79; 95% CI: 0.65–0.92; $p = 0.001$), whereas mechanical HFrec defined by LVEF $\geq 50\%$ was best discriminated by the AECG LVSD score (AUC: 0.94; 95% CI: 0.85–0.99; $p = 5 \times 10^{-5}$). Various AECG parameters relating to R-R interval variability (RRV) and QT interval variability (QTV) differed between controls and HF patients at baseline (Figure 3). Alpha 2, a fractal parameter of RRV, was increased at baseline in HF patients versus controls, but further increased with mental stress only in the controls (Figure 3, top). On the other hand, the RNMSE.T and the root mean square of beat-to-beat QT interval variability in lead II, were not only relatively increased at baseline in the HF patients, but also even more notably increased (further clinically deteriorated) during mental stress in HF patients compared with controls (Figure 3, bottom).

The Empatica E4 output showed both heart rate (HR) and EDA increased with VR-MS in controls (Figure 4); however, only HR rose in HFrEF patients ($p = 0.01$) with accompanying increased QT variability index (QTVi) in

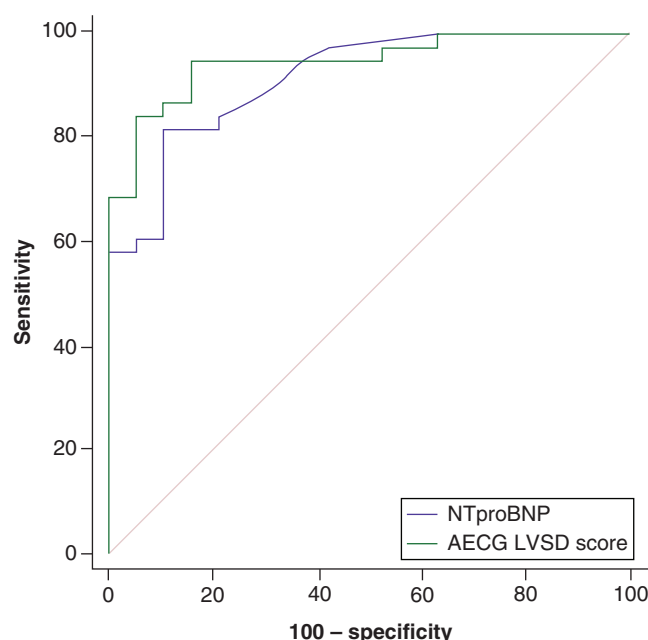


Figure 1. Receiver operating characteristic comparing N-terminal pro hormone BNP and advanced ECG left ventricular systolic dysfunction score for echocardiographic heart failure ejection fraction <50%. AECG: Advanced ECG; LVSD: Left ventricular systolic dysfunction.

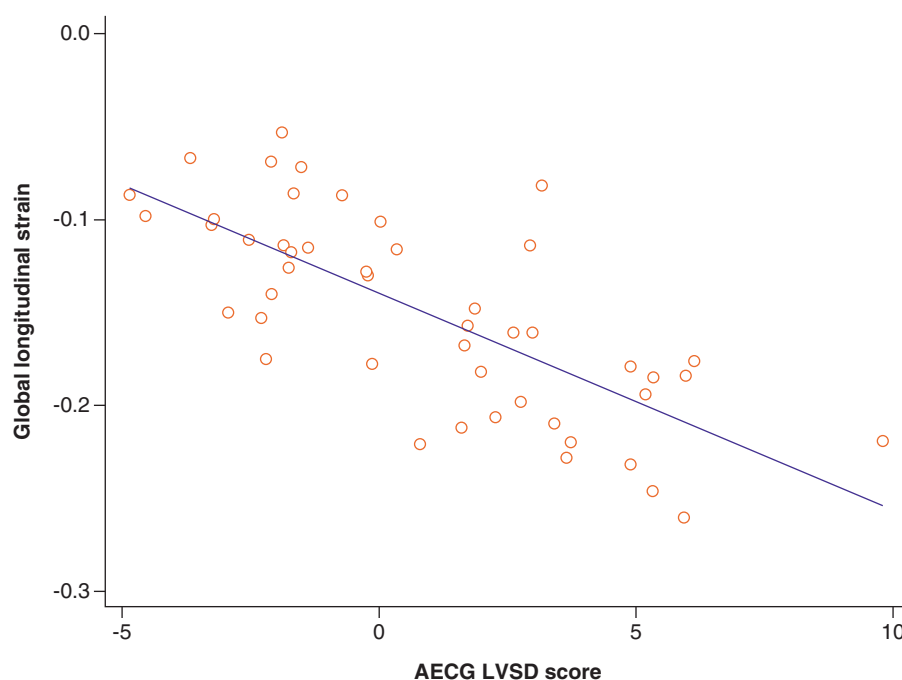


Figure 2. Pearson correlation between global longitudinal strain and advanced ECG left ventricular systolic dysfunction score. AECG: Advanced ECG; LVSD: Left ventricular systolic dysfunction.

those with ICDs ($p = 0.04$). Analysis of the Empatica E4 EDA and PPSG signal with a long short-term memory classifier discriminated between HF and controls prior to and during VR-MS with 81.3 and 73.9% accuracy, respectively. Pulse tonometry analysis was confounded by the presence of atrial fibrillation, including in three of the four *TTN*tv carriers. However, in HFrEF patients without atrial fibrillation compared with controls, central diastolic height was higher, pulse pressure lower and median time between the arrival of the pulse at the artery (the wave foot) and the anacrotic notch (reflected wave arrival) was longer in HFrEF.

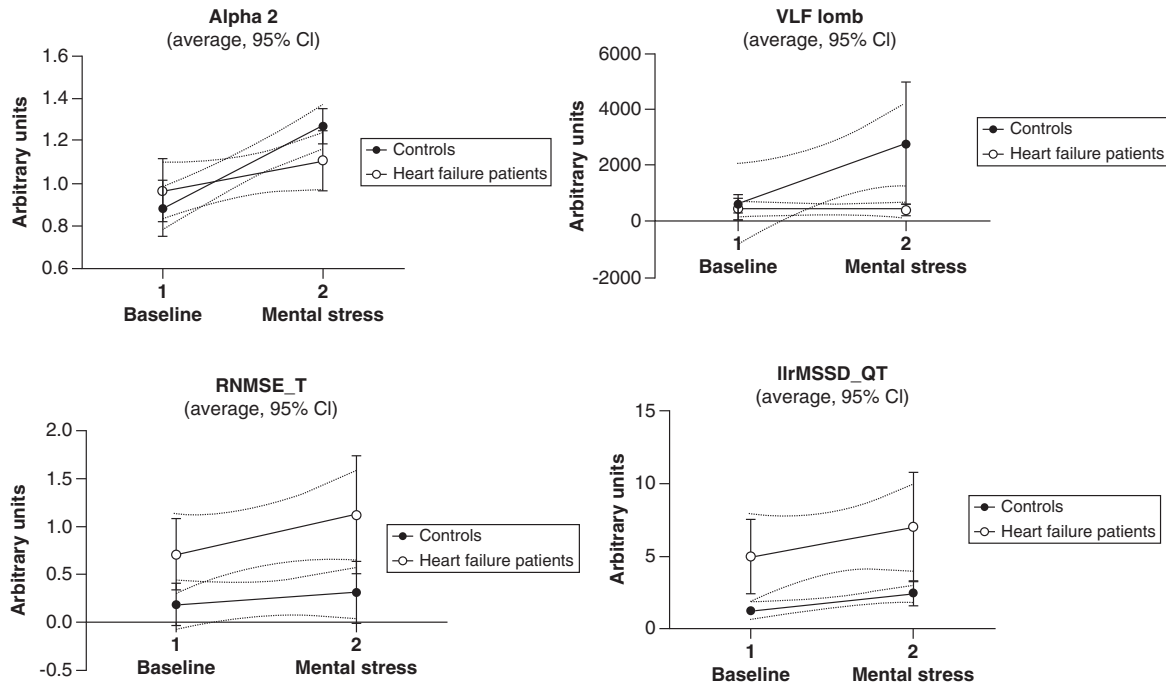


Figure 3. Advanced ECG parameters at baseline and with mental stress. Alpha 2 and VLF power (by Lomb periodogram) of RR interval variability (top panels), and RNMSE.T together with root mean square of beat-to-beat QT interval variability in lead II (IlrMSSD-QT) (bottom panels), before and after mental stress in controls versus heart failure patients. Significantly higher baseline alpha 2 in heart failure patients, along with relatively blunted alpha 2 (and VLF power) responses to mental stress (top panels), suggests relative cardiac sympathetic saturation with depleted cardiac sympathetic reserve at baseline in the heart failure patients. At the same time, both increased baseline and more notable deterioration (increases) in RNMSE.T and IlrMSSD.QT with mental stress suggests reduced electrical coherence in repolarisation with potentially increased ventricular arrhythmic propensity in heart failure patients versus controls (bottom panels). IlrMSSD-QT: Root mean square of beat-to-beat QT interval variability in lead II; RNMSE.T: Root-normalized mean square error of the T wave; VLF: Very low frequency.

Echo AI

Compute time using was < 10 s for classification, segmentation and analysis using a single graphics processing unit (GPU). A total of 11 (18%) nonphysiological AI-ESV and associated AI-LVEF were excluded versus two (3%) manual-LVEF ($\chi^2 = 7$; 95% CI: 3–27; $p = 0.008$). AI generated measurements correlated well with manual measures: LVEDV $r = 0.77$, LVESV $r = 0.8$, LVEF $r = 0.71$, indexed LA volume $r = 0.71$, indexed LV mass $r = 0.6$ and $p < 0.005$. Mean absolute error of M-LVEF versus AI-LVEF was $7.4 \pm 6.6\%$. AI-LVEF, M-LVEF and other HFrEF biomarkers had a similar discrimination for HFrEF (AUC M-LVEF: 0.93 vs AI-LVEF: 0.88; 95% CI: -0.03 to 0.15; $p = 0.19$).

Discussion

In this project we validated a machine learning tool applied to ECG, previously diagnostic for HF and prognostic for related outcomes [5,6]. Second, we developed a pipeline for AI analysis of echocardiography to validate a method for obtaining LVEF more efficiently than manual methods [7]. Third, we integrated this information with next generation sequencing, metabolomics and volatilomics to reveal biological insights and identify novel diagnostic biomarkers (Figure 5). Lastly, we used a wrist worn wearable device and AECG to measure the effect of a VR-MS on a subset of HF patients and controls.

We showed that AECG, using logistic regression scores applied to conventional, spatial (vectorcardiography) and other ECG variables, has a diagnostic accuracy for detecting HF similar to NTproBNP. This result validates this method prospectively, which we have previously shown to have both diagnostic and prognostic value in the context of HFrEF [5,6]. Logistic regression and linear discriminant analysis, both forms of machine learning, applied to detailed ECG segmentation and highly curated databases, underpin the technology [12], which also demonstrates an



Figure 4. Photoplethysmography (top) and pulse wave tonometry (below). Healthy controls; heart rate (PPSG) (top left), heart failure; (top right). Example of Microsoft Aurora output (bottom). PPSG: Photoplethysmography; VR: Virtual reality.

ability to track individual health status over time (Supplementary Figures 1 & 2). This therefore has the transparency and explainability that deep learning methods lack [3,4].

In this study we used AECG to investigate at baseline and during mental stress a number of ECG variables known to be associated with increased arrhythmic risk in HF patients. We showed that not only do patients with HF have increased spatial QRS-T angle at baseline, a biomarker associated with HF readmissions and mortality [6], but also increased alpha 2 RRV fractal dimension [25] and QT variability [26]. Both of these parameters are also strong predictors of mortality that moreover likely indicate, among other things, increased resting efferent cardiac sympathetic activity [25]. During VR-MS, alpha 2 also notably increased in healthy participants, but not in HF patients. The relatively blunted response in alpha 2 in HF patients during mental stress suggests that cardiac sympathetic activity might already be near maximum in such patients, in other words, ‘reduced cardiac sympathetic reserve’. It should also be noted that whereas alpha 2 does not appear to be affected by ‘physical’ stress, for example, postural change [27], it was clearly increased by ‘mental’ stress in healthy subjects in this study. Since alpha 2 of RRV

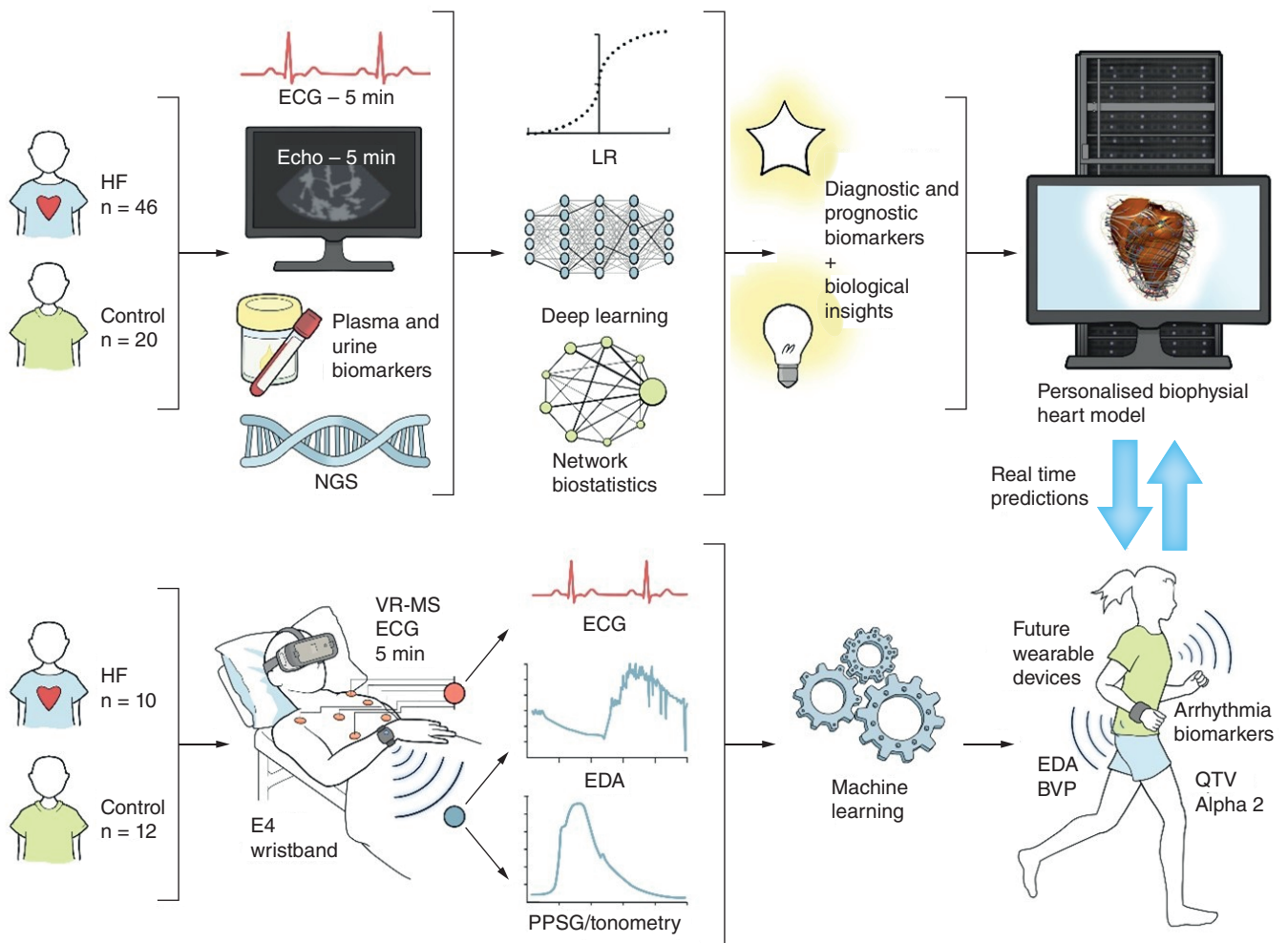


Figure 5. Study workflow, methods and results.

can be derived from single lead ECGs, this finding demonstrates potential promise for employing alpha 2 with wearable technologies to monitor mental stress in patients with and without HF.

We also identified at least two AECG variables, specifically the $RNMSE.T$ and the root mean square of beat-to-beat QT interval variability in lead II, that were not only expectedly increased in HF patients at baseline, but also further relatively increased (worsened) by mental stress in HF patients compared with controls. Pending further validation, variables such as these might therefore hold promise for eventual use with wearable ECG technologies for monitoring arrhythmic propensity in real time.

Our study showed numerous metabolic changes associated with HF, which principally indicated abnormalities in mitochondrial metabolism, namely the citric acid cycle, ketone metabolism and kynurenine pathway. One metabolite, acetone, was validated in the breath of patients with HF using a commercially available sensor. Our study, however, was underpowered to demonstrate any differences in the metabolite profiles of *TTN*tv carriers, particularly as this was confounded by their having a higher NTproBNP. Nor did we observe in *TTN*tv carriers an alteration in urinary N-terminal titin fragments previously shown to be a negative prognostic indicator in HF [28]. We were unable to demonstrate any statistically significant correlations between metabolomic biomarkers and AECG; however, metabolomics has previously shown that kynurenine pathway is associated with mental stress-induced LVSD and ketone bodies (acetate and beta hydroxybutyrate) with QTc in shift workers [29,30]. We were, however, able to show an ability to not only discriminate between healthy participants and HF patients using PPSG and EDA, but also identify the presence of mental stress with a high degree of accuracy. With this

knowledge it may be possible to develop wearable sensors, perhaps also monitoring metabolism [31], which will be capable of predicting HF exacerbations and short-term arrhythmic risk, influenced by mind–heart interactions in real time [32,33].

In our study we validated an Echo AI method provided by Zhang *et al.* [7] and showed that deep learning applied to a 5-min echocardiography protocol rapidly quantifies LVEF, equivalent to human interpretation. This method holds significant utility in the rapid identification of LVSD using POCUS in the ambulatory setting and opens up new opportunities for monitoring and titrating therapies in HF patients. We have previously shown the capability of AECG to identify both structural heart disease and LVSD, and allocate patients to POCUS screening versus full echocardiography [34,35]. Our intention going forward is to integrate all these sources of data into a virtual machine to apply biophysical electromechanical and circulatory computational modeling to better predict outcomes and response to therapies in HF patients [36].

Multimomics has been used fairly extensively in highly controlled cell-based and animal models of disease to identify novel biological pathways or casual genes [37,38]. Due to the high dimensionality and complexity of analysis multimomics is less often used in human studies; however, there is growing expertise in the field which demonstrates it is not only possible but a powerful tool in delivering personalized healthcare, tracking individual responses over time (Supplementary Figure 1). Multimomics has been used to deliver insights into human obesity and prediabetes [39,40]; however, to our knowledge it has not been extensively used in the diagnosis or stratification of human HF [41] or in combination with machine learning applied to echocardiography and ECG [42]. The use of clinical multimomics will be impeded by cost, time and complexity; however, machine learning is the logical tool to assimilate, predict and visualize results in a way which should disburden clinicians who are otherwise awash in data. To a simplistic degree we are working toward the implementation of some of the technologies outlined in this paper in a rapid cardiac screening clinic, using conventional blood tests, ECG and echocardiography ‘omics delivered via a single platform’ [19,20,34,35].

Limitations

This study was small and underpowered to identify metabolomic differences in specific subgroups, for example, *TTN*tv carriers. Multiple hypothesis testing increases the potential for Type I error; however, the discussion has been limited to points for which there is sufficient prior knowledge to make reasonable conclusions.

Conclusion

This study has demonstrated the feasibility of integrating multiple sources of ‘omic clinical data and its potential clinical utility in the context of heart failure. This allowed the expansion of the clinical phenotype of HFrEF suggesting possible future directions for substratifying patients and delivering personalised management strategies. Further work is needed to ensure the additional effort required to generate this data leads to a cost-effective improvement in patient outcomes.

Summary points

- Multimomics holds considerable promise for identifying biological pathways in heart failure (HF), which may have therapeutic or diagnostic (‘theranostic’) potential.
- Breath acetone and other metabolite biomarkers may be useful diagnostic or prognostic tools in human HF.
- Machine learning applied to echocardiography and electrocardiography could be used to expedite and enhance the sensitivity and specificity of these tools to both diagnose and risk stratify patients with HF.
- Deep phenotyping with wearable devices during external perturbation, such as mental stress testing, reveals novel insights into disease pathophysiology.

Supplementary data

To view the supplementary data that accompany this paper please visit the journal website at: www.futuremedicine.com/doi/suppl/10.2217/fca-2020-0225

Author contributions

PA Gladding contributed to ideation of the study, and is the main author. PA Gladding and M Jüllig contributed to statistics of the study. S Loader contributed to research co-ordination, patient enrolment and data collection. E Zarate, S Green and S Villas-

Boas contributed to gas chromatography–mass spectrometry metabolomics and analysis. K Smith, P Shepherd and P Kakadiya contributed to biobanking and next generation sequencing. W Hewitt contributed to echocardiography artificial intelligence coding and data analysis. E Thorstensen, C Keven and M Coe contributed to liquid chromatography–mass spectrometry metabolomics and analysis. B Nakisa, T Vuong and MN Rastgoo contributed to Empatica E4 machine learning analysis. M Jüllig contributed to figures and illustrations. V Starc and T Schlegel contributed to advanced ECG analysis. E Zarate, S Green, S Villas-Boas, B Nakisa, T Vuong, MN Rastgoo, V Starc and T Schlegel contributed to proofing.

Acknowledgments

Authors are thankful to Auckland Regional Tissue Bank. Authors also thank N Rokotyan for data visualisation, and U Holland and V Anderson for study co-ordination.

Financial & competing interests disclosure

This research was funded by a grant from Health Research Council of New Zealand Explorer Grant 16/680. PA Gladding and W Hewitt are cofounders and hold equity in HeartLab AI, a startup company focused on echocardiography artificial intelligence. T Schlegel is the founder and holds equity in Nicollier-Schlegel Sàrl, a provider of advanced ECG services. The authors have no other relevant affiliations or financial involvement with any organization or entity with a financial interest in or financial conflict with the subject matter or materials discussed in the manuscript apart from those disclosed.

No writing assistance was utilized in the production of this manuscript.

Ethical conduct of research

The NanoHF study (A Novel Nanosensor array for Heart Failure diagnosis) was approved by the Northern B Health and Disability Ethics Committee (16/NTB/115) (#16/680) and Waitematā District Health Board's IRB (#RM13458). In addition, for investigations involving human subjects, informed consent has been obtained from the participants involved.

Crown copyright

This work is licensed under Crown copyright protection and licensed for use under the Open Government Licence unless otherwise indicated. Where any of the Crown copyright information in this work is republished or copied to others, the source of the material must be identified and the copyright status under the Open Government Licence acknowledged. Published under CC-BY 4.0 www.nationalarchives.gov.uk/doc/open-government-licence/version/3/ © Crown Copyright.

References

Papers of special note have been highlighted as: ● of interest; ●● of considerable interest

- Jing L, Ulloa Cerna AE, Good CW *et al.* A machine learning approach to management of heart failure populations. *JACC Heart Fail.* 8(7), 578–587 (2020).
- Bayes-Genis A, Liu PP, Lanfear DE *et al.* Omics phenotyping in heart failure: the next frontier. *Eur. Heart J.* 41(36), 3477–3484 (2020).
- **Future perspective of omics in heart failure (HF).**
- Attia ZI, Kapa S, Lopez-Jimenez F *et al.* Screening for cardiac contractile dysfunction using an artificial intelligence-enabled electrocardiogram. *Nat. Med.* 25(1), 70–74 (2019).
- Attia ZI, Kapa S, Yao X *et al.* Prospective validation of a deep learning electrocardiogram algorithm for the detection of left ventricular systolic dysfunction. *J. Cardiovasc. Electrophysiol.* 30(5), 668–674 (2019).
- Johnson K, Neilson S, To A *et al.* Advanced electrocardiography identifies left ventricular systolic dysfunction in non-ischemic cardiomyopathy and tracks serial change over time. *J. Cardiovasc. Dev. Dis.* 2(2), 93–107 (2015).
- Gleeson S, Liao YW, Dugo C *et al.* ECG-derived spatial QRS-T angle is associated with ICD implantation, mortality and heart failure admissions in patients with LV systolic dysfunction. *PLoS ONE* 12(3), e0171069 (2017).
- **Details prognostic value of advanced ECG in HF.**
- Zhang J, Gajjala S, Agrawal P *et al.* Fully automated echocardiogram interpretation in clinical practice. *Circulation* 138(16), 1623–1635 (2018).
- **First description of deep learning applied to echocardiography.**
- Madani A, Arnaout R, Mofrad M, Arnaout R. Fast and accurate view classification of echocardiograms using deep learning. *NPJ Digital Medicine* 1(1), 6 (2018).
- Ghorbani A, Ouyang D, Abid A *et al.* Deep learning interpretation of echocardiograms. *NPJ Digital Medicine* 3(1), 10 (2020).
- Luong C, Abdi A, Jue J *et al.* Abstract 17562: automatic quality assessment of echo apical 4-chamber images using computer deep learning. *Circulation* 134(Suppl. 1), A17562–A17562 (2016).

11. Stehlik J, Schmalfuss C, Bozkurt B *et al.* Continuous wearable monitoring analytics predict heart failure hospitalization. *Circ.: Heart Failure* 13(3), e006513 (2020).
12. Schlegel TT, Kulecz WB, Feiveson AH *et al.* Accuracy of advanced versus strictly conventional 12-lead ECG for detection and screening of coronary artery disease, left ventricular hypertrophy and left ventricular systolic dysfunction. *BMC Cardiovasc. Disord.* 10(1), 28 (2010).
- **Details advanced ECG method and validation.**
13. Maruyama N, Asai T, Abe C *et al.* Establishment of a highly sensitive sandwich ELISA for the N-terminal fragment of titin in urine. *Sci. Rep.* 6, 39375 (2016).
14. Batdorf BH, Feiveson AH, Schlegel TT. The effect of signal averaging on the reproducibility and reliability of measures of T-wave morphology. *J. Electrocardiol.* 39(3), 266–270 (2006).
15. Kors JA, van Herpen G, Sittig AC, van Bommel JH. Reconstruction of the Frank vectorcardiogram from standard electrocardiographic leads: diagnostic comparison of different methods. *Eur. Heart J.* 11(12), 1083–1092 (1990).
16. Rautaharju PM, Kooperberg C, Larson JC, LaCroix A. Electrocardiographic predictors of incident congestive heart failure and all-cause mortality in postmenopausal women: the women's health initiative. *Circulation* 113(4), 481–489 (2006).
17. Starc V, Swenne CA. Spatial distribution and orientation of a single moving dipole computed in 12-lead ECGs of a healthy population using a spherically bounded model. In: *2017 Computing in Cardiology (CinC)*. 1–4 (2017). <https://ieeexplore.ieee.org/document/8331644>
18. Starc V, Schlegel TT. Real-time multichannel system for beat-to-beat QT interval variability. *J. Electrocardiol.* 39(4), 358–367 (2006).
19. Gladding P, Cave A, Zareian M *et al.* Open access integrated therapeutic and diagnostic platforms for personalized cardiovascular medicine. *J. Pers. Med.* 3(3), 203 (2013).
20. Hussan JR, Hunter PJ, Gladding PA *et al.* ICMA: an integrated cardiac modeling and analysis platform. *Bioinformatics* 31(8), 1331–1333 (2015).
21. Zimmer P, Buttlar B, Halbeisen G, Walther E, Domes G. Virtually stressed? A refined virtual reality adaptation of the Trier Social Stress Test (TSST) induces robust endocrine responses. *Psychoneuroendocrinology* 101, 186–192 (2019).
22. Jonsson P, Wallergard M, Osterberg K, Hansen AM, Johansson G, Karlson B. Cardiovascular and cortisol reactivity and habituation to a virtual reality version of the Trier Social Stress Test: a pilot study. *Psychoneuroendocrinology* 35(9), 1397–1403 (2010).
23. Kazzi C, Blackmore C, Shirbani F *et al.* Effects of instructed meditation augmented by computer-rendered artificial virtual environment on heart rate variability. Conference proceedings: . . . Annual International Conference of the IEEE Engineering in Medicine and Biology Society. IEEE Engineering in Medicine and Biology Society. *Annual Conference* 2018, 2768–2771 (2018).
24. Lampert R. ECG signatures of psychological stress. *J. Electrocardiol.* 48(6), 1000–1005 (2015).
25. Piccirillo G, Magri D, Ogawa M *et al.* Autonomic nervous system activity measured directly and QT interval variability in normal and pacing-induced tachycardia heart failure dogs. *J. Am. Coll. Cardiol.* 54(9), 840–850 (2009).
- **Well powered study evaluating metabolomics in HF.**
26. Baumert M, Porta A, Vos MA *et al.* QT interval variability in body surface ECG: measurement, physiological basis, and clinical value: position statement and consensus guidance endorsed by the European Heart Rhythm Association jointly with the ESC Working Group on Cardiac Cellular Electrophysiology. *Europace* 18(6), 925–944 (2016).
27. de Souza AC, Cisternas JR, de Abreu LC *et al.* Fractal correlation property of heart rate variability in response to the postural change maneuver in healthy women. *Int. Arch. Med.* 7, 25–25 (2014).
28. Yoshihisa A, Kimishima Y, Kiko T *et al.* Usefulness of urinary N-terminal fragment of titin to predict mortality in dilated cardiomyopathy. *Am. J. Cardiol.* 121(10), 1260–1265 (2018).
29. Boyle SH, Matson WR, Velazquez EJ *et al.* Metabolomics analysis reveals insights into biochemical mechanisms of mental stress-induced left ventricular dysfunction. *Metabolomics* 11(3), 571–582 (2015).
30. Campagna M, Locci E, Piras R *et al.* Metabolomic patterns associated to QTc interval in shiftworkers: an explorative analysis. *Biomarkers* 21(7), 607–613 (2016).
31. Yokokawa T, Sato T, Suzuki S *et al.* Feasibility of skin acetone analysis in patients with cardiovascular diseases. *Fukushima J. Med. Sci.* 64(2), 60–63 (2018).
32. Cho D, Ham J, Oh J *et al.* Detection of stress levels from biosignals measured in virtual reality environments using a kernel-based extreme learning machine. *Sensors (Basel)* 17(10), 1–18 (2017).
33. Chiu H-C, Lin Y-H, Lo M-T *et al.* Complexity of cardiac signals for predicting changes in alpha-waves after stress in patients undergoing cardiac catheterization. *Sci. Rep.* 5(1), 13315 (2015).
34. Gladding P, Schlegel T, Walsh H, Dawson L, O'Shaughnessy B, Scott T. Screening low risk patients referred for echocardiography with a 5-min scout and advanced electrocardiography. *Heart, Lung and Circulation* 26, S28 (2017).
35. Gladding P, Dugo C, Wynne Y *et al.* Screening for cardiac disease with genetic risk scoring, advanced ECG, echocardiography, protein biomarkers and metabolomics. *Heart, Lung Circ.* 27, S8 (2018).

36. Hunter P. The virtual physiological human: the physiome project aims to develop reproducible, multiscale models for clinical practice. *IEEE Pulse* 7(4), 36–42 (2016).
37. Joshi A, Rienks M, Theofilatos K, Mayr M. Systems biology in cardiovascular disease: a multiomics approach. *Nat. Rev. Cardiol.* 18, 313–330 (2021).
38. Santolini M, Romay MC, Yukhtman CL *et al.* A personalized, multiomics approach identifies genes involved in cardiac hypertrophy and heart failure. *NPJ Syst. Biol. Appl.* 4(1), 12 (2018).
39. Piening BD, Zhou W, Contrepois K *et al.* Integrative personal omics profiles during periods of weight gain and loss. *Cell Systems* 6(2), 157–170.e158 (2018).
40. Zhou W, Sailani MR, Contrepois K *et al.* Longitudinal multi-omics of host-microbe dynamics in prediabetes. *Nature* 569(7758), 663–671 (2019).
41. Bayes-Genis A, Liu PP, Lanfear DE *et al.* Omics phenotyping in heart failure: the next frontier. *Eur. Heart J.* 41(36), 3477–3484 (2020).
- **Detailed multiomics analysis in prediabetes.**
42. Andersson C, Lin H, Liu C *et al.* Integrated multiomics approach to identify genetic underpinnings of heart failure and its echocardiographic precursors: Framingham heart study. *Circ. Genom. Precis. Med.* 12(12), e002489 (2019).